Hindawi Publishing Corporation
Mathematical Problems in Engineering
Volume 2012, Article ID 710690, 16 pages
doi:10.1155/2012/710690

Research Article

Automatic Regulation Time Series for Industry Processes

Tain-Sou Tsay

Department of Aeronautical Engineering, National Formosa University, Huwei, Yunlin 63208, Taiwan

Correspondence should be addressed to Tain-Sou Tsay, tstsay@nfu.edu.tw

Received 28 January 2012; Accepted 20 March 2012

Academic Editor: Ming Li

A nonlinear digital control scheme is proposed for analyses and designs of stable industry processes. It is derived from the converging characteristic of a specified numerical time series. The ratios of neighbourhoods of the series are formulated as a function of the output of the plant and the reference input command and will be converted to be unities after the output has tracked the reference input command. Lead compensations are also found by another numerical time series to speed up the system responses on the online adjusting manner. A servosystem, a time-delay system, a high-order system, a very-high-order system, and a 2×2 multivariable aircraft gas turbine engine are used to illustrate effectiveness of the proposed nonlinear digital controller. Comparisons with other conventional methods are also made.

1. Introduction

For unit feedback discrete-time control systems, the control sequences are usually functions of the difference between the sampled reference input and output of the plant [1–5]. The discrete-time control sequence can be generated by Finite Impulse Response (FIR) filter or Infinite Impulse Response (IIR) filter. The input of FIR or IIR filter is the difference between the sampled reference input and output of the plant. The output of FIR or IIR will be the input of the plant. In general, they are linear controllers.

In this literature, a nonlinear discrete-time control sequence described by periodic numerical series $G(jT_S)$ is proposed for analyses and designs of industry processes. They are sampled-data feedback control systems. T_S represents the sampling interval. The ratios of $G((k+1)T_S)$ to $G(kT_S)$ of the series are formulated as a function of the reference input command and the output of the plant. The value of $G(kT_S)$ is the control input of the plant at time intervals between $(k-1)T_S$ and kT_S. Thus, the considered system is closed as a feedback control system by use of $G(jT_S)$. It will be seen that the output of the plant tracks the reference

input command exactly after ratios $G((k+1)T_S)/G(kT_S)$ of the series being converted to unities. It implies that $G(kT_S)$ will be converted to a steady-state value for a constant reference input applied. The stability of the closed-loop system is guaranteed by selecting the proper function of ratios $G((k+1)T_S)/G(kT_S)$. This function can be called as "Regulation Function." It will be proven that the considered system using $G(kT_S)$ becomes a negative feedback control system for a stable plant [4].

Note that it needs not integration to get zero tracking error, and performance of controlled systems are dependent on selected functions of $G((k+1)T_S)/G(kT_S)$. Furthermore, an adaptive limitation for $G(kT_S)$ can be applied also to minimize the control effort and get better performance. Controlled results will be compared with conventional famous PI and PID controllers [6–15]. In this work, measurement noises of plant outputs are not considered. It is worthwhile to include recent developments of fractional-order systems and controls [16, 17] in the proposed nonlinear automatic regulation time series. They have been applied to signal processing [18], Cyber-physical networking system [19, 20], PMSM position servo system [21], and optimal control [22].

In following sections, basic concepts of the proposed nonlinear discrete-time control sequence are discussed first, and then a servo system, a time-delay system, a high-order system, a very-high-order system, and a 2×2 multivariable aircraft gas turbine examples are used to illustrate their tracking behaviour and performance. Simulating results will show that the proposed nonlinear digital controller gives another possible way for analyses and designs of industry processes. Design results of the fourth example give the proposed method can also be applied to multivariable feedback control systems.

2. The Basic Approach

2.1. Automatic Regulation Time Series

A numerical series with time interval T_S [1–5] can be written as in the form of

$$G(jT_S), \quad j = 1, 2, 3, \ldots, n, n+1, \ldots, \tag{2.1}$$

where $G(jT_S)$ represents a constant value between time interval from $(j-1)T_S$ and jT_S. For simplicity, the representation of $G(jT_S)$ will be replaced by $G(j)$ in the following evaluations. The ratios $G(j+1)/G(j)$ of the series are defined as in the form of

$$F(j) = \frac{G(j+1)}{G(j)}, \quad j = 1, 2, 3, \ldots, n, n+1, \ldots. \tag{2.2}$$

Equation (2.2) gives the value of $G(n+1)$ approaches to be a constant value when the value of $F(n)$ approaches to be unity. Now, the problem for closing the considered system is to find the formula of $F(j)$ which is the function of the reference input command R and the output of the plant Y. $G(n+1)$ is used as the input of the considered system. Considering a series given below,

$$G(n+1) = \left[\sum_{i=0}^{m} a_i \left(\frac{R(n)}{Y_S(n)}\right)^i\right] G(n), \tag{2.3}$$

where $R(n)$ represents the reference input command and $Y_S(n)$ represents the nonzero sampled output of the plant at the sampling interval nT_S. Note that this non-zero constraint will be removed later by level shifting. Equation (2.3) is a possible way to close the considered system as a sampled-data feedback control system. Assuming the reference input command has been tracked by applying control effort $G(j)$, (2.3) becomes

$$G(n+1) = \sum_{i=0}^{m} a_i G(n). \tag{2.4}$$

For steady-state condition, $G(n+1)$ approaches to be a constant value, and it gives

$$\sum_{i=0}^{m} a_i = 1. \tag{2.5}$$

Rearranging (2.3) and taking the derivative of it with respect to $Y_S(n)/R(n)$, one has

$$F(n) = \sum_{i=0}^{m} a_i \left(\frac{Y_S(n)}{R(n)} \right)^{-i}, \tag{2.6}$$

$$\frac{\partial F(n)}{\partial (Y_S(n)/R(n))} = -\sum_{i=0}^{m} i a_i \left(\frac{Y_S(n)}{R(n)} \right)^{-1-i}. \tag{2.7}$$

The sufficient but not necessary condition for (2.7) less than zero is $a_i > 0$ for $Y_S(n)/R(n) \cong 1$ and (2.6) can be rewritten as in the form of

$$F(n) = \sum_{i=0}^{m} a_i \left| \frac{Y_S(n)}{R(n)} \right|^{-i}. \tag{2.8}$$

$a_i > 0$ will be used in the following evaluations. Negative value of (2.7) represents the closed-loop system using (2.3) activated as a negative feedback system around the equilibrium condition; that is, $Y_S(n) = R(n)$. This statement will be illustrated and discussed by a graph in the next paragraph. The first-order polynomial described in (2.3) can be written as in the form of

$$G(n+1) = \left[\beta \left| \frac{R(n)}{Y_S(n)} \right| + 1 - \beta \right] G(n), \tag{2.9}$$

where β satisfies constrains stated above and becomes an adjustable parameter. Thus, the ratios $F(n)$ become

$$F(n) = \beta \left| \frac{R(n)}{Y_S(n)} \right| + 1 - \beta. \tag{2.10}$$

$F(n)$ can be called as "Regulation Function" also. Similarly, the third-order representation of $F(n)$ is in the form of

$$F(n) = \alpha \left| \frac{Y_S(n)}{R(n)} \right|^{-3} + \gamma \left| \frac{Y_S(n)}{R(n)} \right|^{-1} + 1 - \alpha - \gamma, \tag{2.11}$$

where $0 < \alpha$ and $0 < \gamma$.

Taking the derivative of (2.10) with respect to $Y_S(n) = R(n)$, one has

$$\frac{\partial F(n)}{\partial (Y_S(n)/R(n))} = -\beta \left(\frac{Y_S(n)}{R(n)} \right)^{-2}. \tag{2.12}$$

For negative value of (2.12), the value of β must be greater than zero. This implies the range of β is $0 < \beta < 1$. The suitability of the proposed nonlinear adaptive digital controller is based on this negative regulation characteristic. Figure 1 shows ratios $F(n)$ versus $R(n)/Y_S(n)$ represented by (2.9) for $\beta = 0.9, 0.7, 0.5, 0.3$ and 0.1, respectively.

Figure 1 shows that the value of $F(n)$ is less than one for that of $Y_S(n)$ greater than that of $R(n)$, then the value of $G(n+1)$ will be decreased; the value of $F(n)$ is greater than one for that of $Y_S(n)$ less than that of $R(n)$, and the value of $G(n+1)$ will be increased. This implies that the controlled system connected using (2.9) will be regulated to the equilibrium point $(Y_S(n)/R(n) = 1)$ and gives a negative feedback control system for deviation from the equilibrium point. From Figure 1, it can be seen that one can adjust β to get desired regulating slope; that is, regulating characteristic. Certainly, other tracking functions can be formulated and proposed also for the considered system, if its derivative with respect to $Y_S(n)/R(n)$ is negative. Similar to the derivation of (2.12), (2.11) gives

$$\frac{\partial F(n)}{\partial (Y_S(n)/R(n))} = -\left\{ \gamma \left(\frac{Y_S(n)}{R(n)} \right)^{-2} + 3\alpha \left(\frac{Y_S(n)}{R(n)} \right)^{-4} \right\}, \tag{2.13}$$

where $0 < \alpha$ and $0 < \gamma$.

The constraint of non-zero $Y_S(n)$ can be removed by $R(n)/Y_S(n)$ of (2.9) replaced by $(R(n) + Y_o)/(Y_S(n) + Y_o)$. Y_o is a positive value and represents the negative maximal control swing. The modified equation of (2.9) becomes

$$G(n+1) = \left\{ \beta \left| \frac{R(n) + Y_o}{Y_S(n) + Y_o} \right| + 1 - \beta \right\} G(n). \tag{2.14}$$

Equation (2.14) implies ratios $G(n+1)/G(n)$ are in the form of

$$F(n) = \left[\beta \left| \frac{R(n) + Y_o}{Y_S(n) + Y_o} \right| + 1 - \beta \right], \quad n = 1, 2, 3, \ldots, j, j+1, \ldots. \tag{2.15}$$

Control inputs of the plant are in the form of

$$u(n+1) = G(n+1) - \frac{Y_o}{P(0)} \tag{2.16}$$

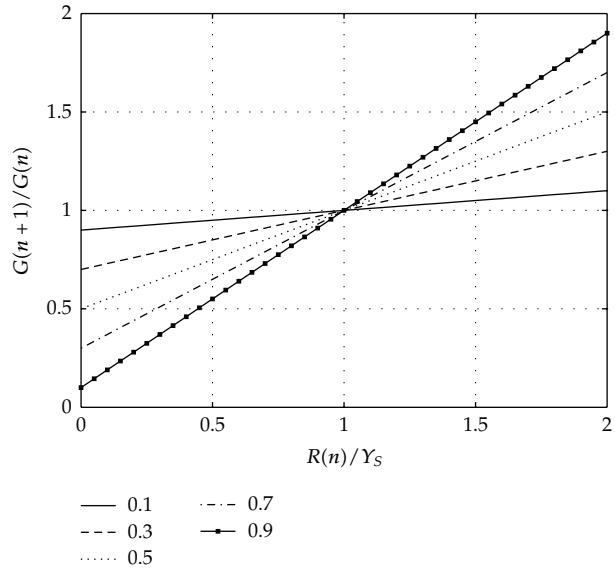

Figure 1: $G(n+1)/G(n)$ Versus R/Y_S for $\beta = 0.9, 0.7, 0.5, 0.3$, and 0.1.

for the negative swing control using positive values of β, $G(n)$, and $F(n)$. Equation (2.14) gives negative regulation characteristics also for $R(n) = Y_S(n)$ is corresponding to $R(n)+Y_o = Y_S(n) + Y_o$. Similar to the evaluation of (2.12), the derivative of (2.15) becomes

$$\frac{\partial F(n)}{\partial((Y_S(n)+Y_o)/(R(n)+Y_o))} = -\beta\left(\frac{Y_S(n)+Y_o}{R(n)+Y_o}\right)^{-2}. \tag{2.17}$$

Figure 2 shows the connected system configuration using (2.14) and (2.16) in which U is the sampled with hold output of the controller. The values of $G(n)$ and $F(n)$ will be all positive for the summation of $Y_S(n)$ and Y_o (or R and Y_o) is greater than zero with specified values of Y_o. All positive values will give the better continuity and regulating characteristic of the time series. Naturally, absolute value of $(R(n)+Y_o)/(Y_S(n)+Y_o)$ can be used in (2.14) to guarantee positive of $G(n)$ and $F(n)$ for negative of $R(n)$.

2.2. Control Effort Limitation

An adaptive value of Y_o can be selected at $|R(n)|$ for the system is well controlled. Then (2.14) and (2.16) can be rewritten as

$$G(n+1) = \left\{\beta\left|\frac{R(n)+|R(n)|}{Y_S(n)+|R(n)|}\right| + 1 - \beta\right\}G(n), \tag{2.18}$$

$$u(n+1) = G(n+1) - \frac{|R(n)|}{P(0)}, \tag{2.19}$$

respectively. The maximal value of $G(n)$ can be limited by an adaptive constraint $|R(n) + |R(n)||$ to minimize the control effort. The control input U of the plant is now described by (2.19).

Note that the singularity of (2.18) must be avoided when $Y_S(n) + |R(n)| = 0$. It is easy to replace $Y_S(n) + |R(n)| = 0$ by a small value. A small value of $G(n)$ is selected also to avoid null time series. Figure 3 shows an equivalent block diagram of Figure 2 using constraint of $G(n)$ and singularity avoidance of $Y_S(n) + |R(n)| = 0$. The constrain of $G(n)$ cannot be only for minimizing the control effort but also for improving system performance.

2.3. Phase Lead Compensation

A conventional digital filter $C(z)$ in Figure 3 can be applied for filtering $G(n)$, if it is necessary. In general, phase lead is used for speeding up the time response. The first-order phase lead can be expressed as

$$C(z) = \left.\frac{T_n s + 1}{T_n s/\rho + 1}\right|_{s=(2/T_S)((z-1)/(z+1))} \tag{2.20}$$

for $\rho > 1$. The parameter T_n can be found by another numerical time series. It is

$$\begin{aligned} W(n+1) &= \left[\eta\left(\frac{T_c}{T_{cs}}\right)^j + 1 - \eta\right] W(n), \\ T_n &= W(n+1), \end{aligned} \tag{2.21}$$

where T_c is the time constant of the closed loop system and T_{cs} is the wanted time constant.

Considering a illustrating example [6] is shown in Figure 3, in which $P(s)$ is in the form of

$$P(s) = \frac{30}{s^2 + 10s + 30}. \tag{2.22}$$

DC gain of $P(s)$ is unity. The sampling period T_S is selected to be equal to 0.1 second for illustrating variations of $G(n)$ and $F(n)$. Time responses of the overall system using the nonlinear digital controller for $\beta = 0.5$, $Y_o = |R(n)|$ and $C(z) = 1$ are shown in Figure 4. Magnitudes of reference inputs between 0 and 5 seconds are equal to 1, between 5 and 10 seconds are equal to −0.7, between 10 and 14 seconds are equal to 0.5, and between 14 and 17 seconds are equal to −0.3, in which gives reference input $R(n)$ (dash line), output Y (solid line), time series $G(n)$ (dotted line), and ratios $F(n)$ (dash-dotted line) of $G(n)$. Figure 4 shows that all values of $G(n)$ and $F(n)$ are positive while the value of output Y is tracking the negative value of the reference input $R(n)$. The value of $R(n)$ can be positive or negative.

Figure 4 shows also that ratios $F(n)$ are converted to be unities quickly; that is, the controlled output tracks the reference input quickly. The proposed method gives a good performance and zero steady-state error without integration. Note that maximal values of $G(n)$ are set to be $|R(n) + |R(n)||$ for better performance and minimal the control effort. Equation (2.14) gives that $F(n)$ will be converted to 0.5 for zero input ($R(n) = 0$) and $\beta = 0.5$. Equation (2.14) and Figure 1 give that the less the value of β is, the larger the regulation slope will be. $\beta = 0.5$ is the optimal value for the considered system.

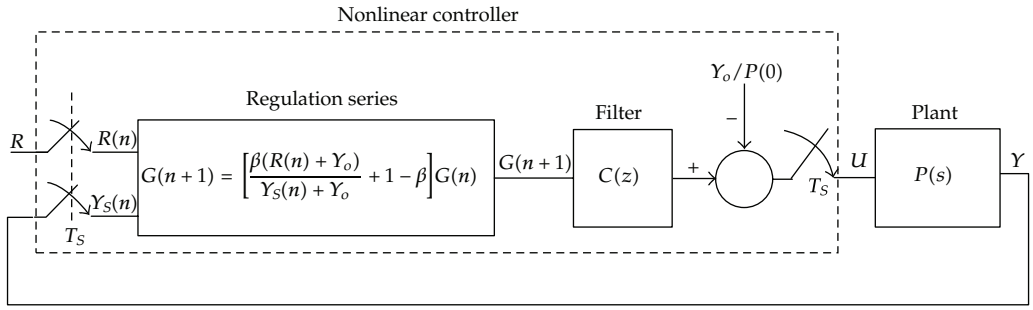

Figure 2: A nonlinear digital controller using automatic regulation time series.

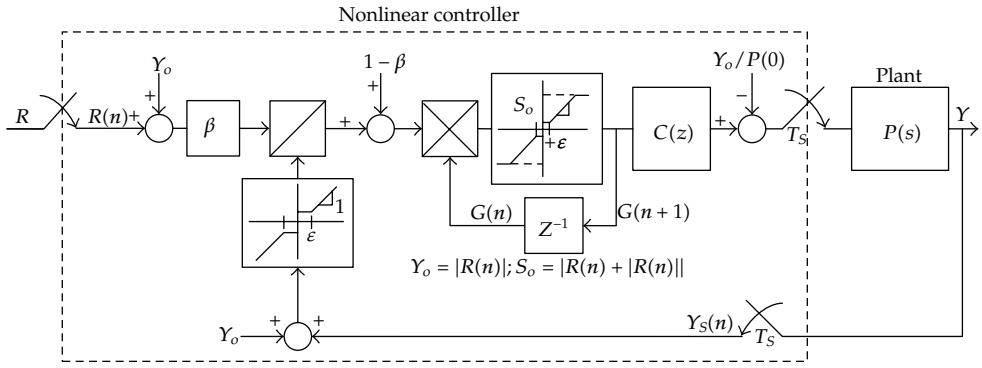

Figure 3: Equivalent block diagram of Figure 2 using $G(n)$ limitations and singularity avoidance of (2.18).

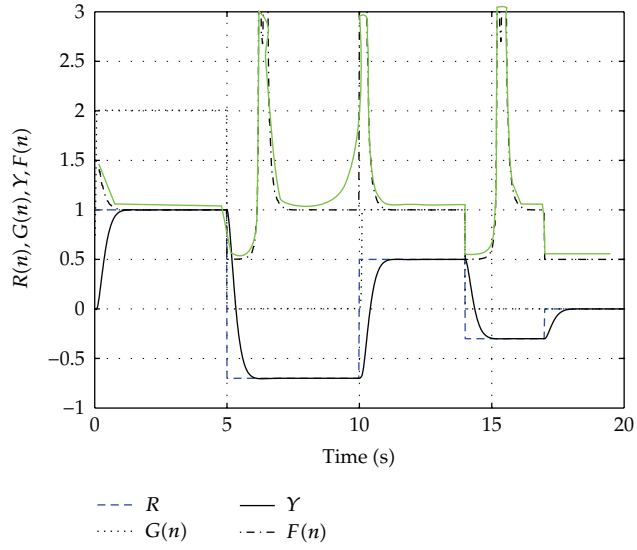

Figure 4: Time responses of the illustrating example for $\beta = 0.50$ and $T_S = 0.1$ sec.

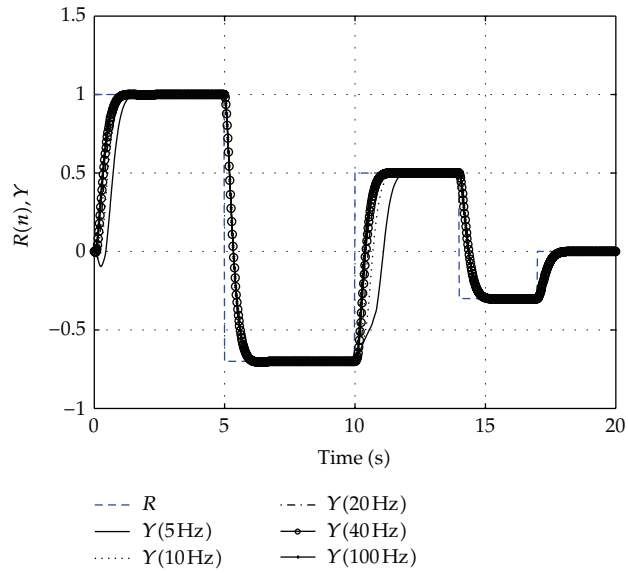

Figure 5: Time responses of the illustrating example for $\beta = 0.50$ and *sampling frequency* equating to 100, 40, 20, 10, and 5 Hz, respectively.

Figure 5 shows time responses for $\beta = 0.50$ and sampling frequency equal to 100, 40, 20, 10, and 5 Hz, respectively. It shows that 40 Hz (i.e., $T_S = 25$ ms) is fast enough for the considered system. Figure 6 shows comparisons with a phase-lead compensator $C(z)$ which is included in the control loop. The phase-lead compensator $C(z)$ is in the form of

$$C(z) = \left.\frac{0.15923s + 1}{0.03185s + 1}\right|_{s = (2/T_S)((z-1)/(z+1))}. \tag{2.23}$$

It can speed up the time responses while keeping system performance.

The proposed control scheme using numerical time series will be applied to three numerical SISO (single-input single-output) examples in next section on online adjusting manner. Equation (2.21) will be used for finding phase-lead compensators $C(z)$ to meet design specifications.

3. Numerical Examples

Example 3.1. Consider a stable plant that has the transfer function [7, 8]

$$P_1(s) = \frac{e^{-s}}{(s+1)^2}. \tag{3.1}$$

It has pure time delay of 1 second. The specification for time constant $T_{cs} = 1.85$ sec is selected. Parameters of (2.18) and (2.21) are $\beta = 0.7$, $T_S = 25$ ms, $\rho = 50$, $\eta = 0.9$, and $j = 1$. Figure 7

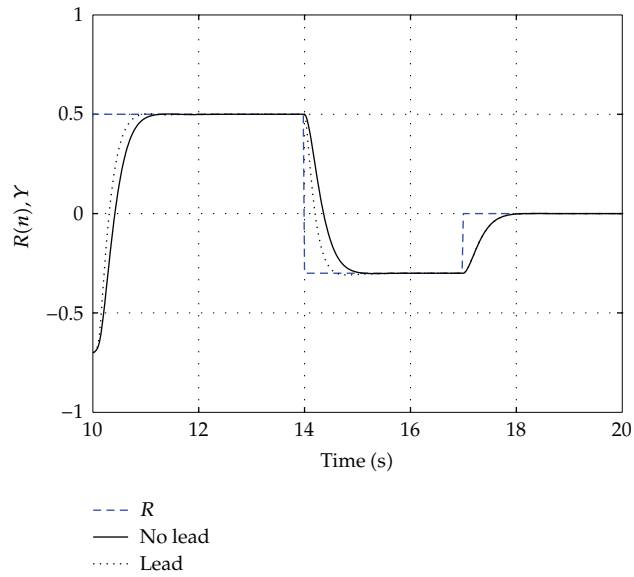

Figure 6: Time responses of the illustrating example with/without $C(z)$ for $\beta = 0.5$, $T_S = 25$ ms.

shows online adjusting processes for finding $C(z)$. The initial guess of T_n is equal to 1.00 and converted to 0.5195 after third adjusting processes. The found lead compensator is

$$C(z) = \left.\frac{0.5195s + 1}{0.5195s/\rho + 1}\right|_{s=(2/T_S)((z-1)/(z+1))}. \tag{3.2}$$

Time constants of each step are 1.4107, 1.8488, 1.8498, and 1.8500. Figure 7 shows the proposed method provides an automatic regulation procedure to get wanted design specifications. It gives good performance and zero steady-state error.

Simulation results of the proposed method and four other methods are presented for comparisons. They are Ziegler-Nichols method [9–12] for finding PI and PID compensators, Tan et al. [13, 14] for finding PID compensator, and Majhi [7, 8] for finding PI compensator. The controller is in the form of

$$u(t) = K_p e(t) + K_i \int e(t)dt + K_d \frac{d}{dt} e(t). \tag{3.3}$$

Parameters of four found compensators are given below:

(1) ZN(PI): $K_p = 1.240$ and $K_i = 0.251$;

(2) ZN(PID): $K_p = 1.6367$, $K_i = 0.4187$, and $K_d = 0.5972$;

(3) Tan's(PID): $K_p = 0.620$, $K_i = 0.5636$, and $K_d = 0.1705$;

(4) Majhi's(PI): $K_p = 0.864$ and $K_i = 0.3653$.

Integral of the Square Error (ISE) and Integral of the Absolute Error (IAE) are given in Table 1. Time responses are shown in Figure 8. From Table 1 and Figure 8, one can see that the proposed method gives faster and better performance than those of other methods presented.

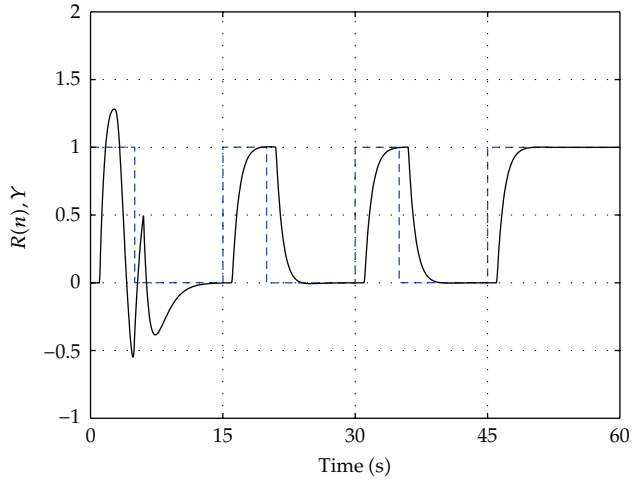

Figure 7: Time responses of Example 3.1 for finding $C(z)$.

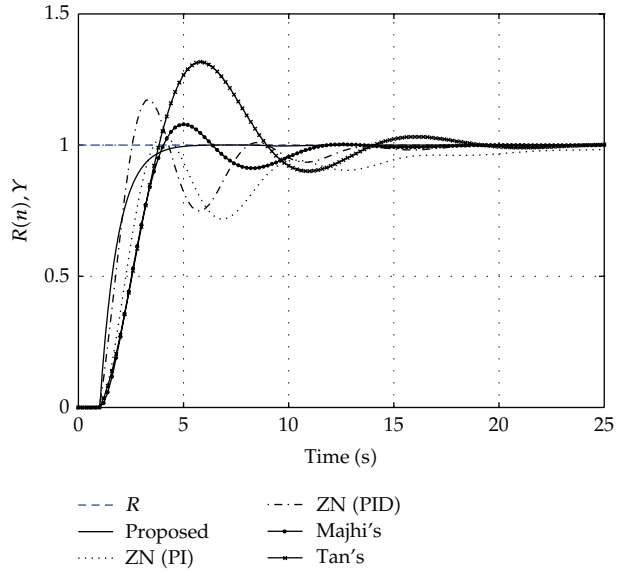

Figure 8: Time responses of Example 3.1 using different control methods.

Table 1: IAE and ISE errors of Example 3.1 using different control methods.

Methods	Proposed	ZN(PI)	ZN(PID)	Tan's	Majhi's
ISE	1.4610	2.2675	1.7694	2.2471	2.4654
IAE	1.8726	4.0107	2.8757	3.0725	4.0659

Example 3.2. Consider a sixth order plant [7, 8]

$$P_2(s) = \frac{1}{(s+1)^6}. \tag{3.4}$$

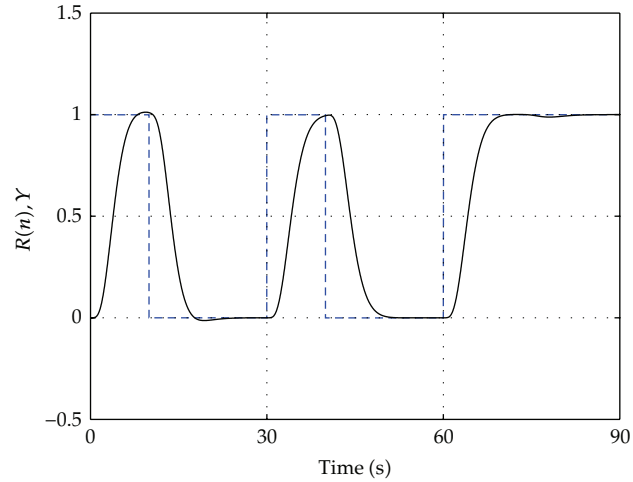

Figure 9: Time responses of Example 3.2 for finding $C(z)$.

Table 2: IAE and ISE errors of Example 3.2 using different control methods.

Methods	Proposed	ZN(PI)	ZN(PID)	Ho's	Majhi's
ISE	3.3895	5.335	4.023	5.215	3.746
IAE	4.4798	9.279	6.492	7.219	5.425

The specification of time constant $T_{cs} = 4.8$ sec is selected. Parameters of (2.18) and (2.21) are $\beta = 0.5$, $T_S = 25$ ms, $\rho = 50$, $\eta = 0.9$, and $j = 3$. The initial guess of T_n is equal to 1.0 and converted to 0.7759 after second adjusting process. The found lead compensator is

$$C(z) = \left.\frac{0.7759s + 1}{0.7759s/\rho + 1}\right|_{s=(2/T_S)((z-1)/(z+1))}. \tag{3.5}$$

Figure 9 shows on-line adjusting processes for finding $C(z)$ to meet $T_{cs} = 4.8$ sec. Simulation results of the proposed and four other methods are presented for comparisons. They are Ziegler-Nichols rule [9–12] for finding PI and PID compensators, Ho et al. [15] for finding PID compensator, and Majhi [7, 8] for finding PI compensator. Parameters of five found compensators are given below:

(1) ZN(PI): $K_p = 1.079$ and $K_i = 0.110$;

(2) ZN(PID): $K_p = 1.4248$, $K_i = 0.1838$, and $K_D = 1.360$;

(3) Majhi's(PI): $K_p = 0.7736$, and $K_i = 0.1547$;

(4) Ho's(PID): $K(s) = 1.3(1 + 0.189/s + 1.3s/(0.13s + 1))$.

Integral of the Square Error (ISE) and Integral of the Absolute Error (IAE) are given in Table 2. Time responses are shown in Figure 10. From Table 2 and Figure 10, one can see that the proposed method gives faster and better performance than those of other methods.

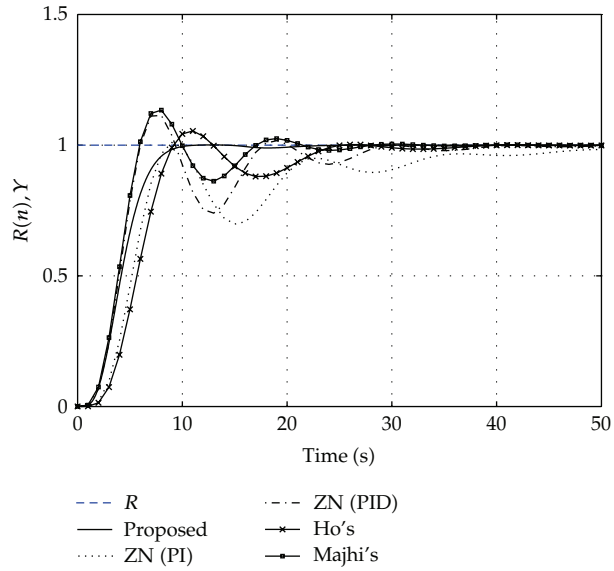

Figure 10: Time responses of Example 3.2 using different control methods.

Example 3.3. Consider the very-high-order plant [7, 8]:

$$P_3(s) = \frac{1}{(s+1)^{20}}. \tag{3.6}$$

The design specification for time constant $T_{cs} = 19.0$ sec is selected. Parameters of (2.18) and (2.21) are $\beta = 0.5$, $T_S = 25$ ms, $\rho = 50$, $\eta = 0.9$, and $j = 3$. The initial guess of T_n is equal to 1.00 and converted to 0.9586 after the fourth adjusting process. The found lead compensator is

$$C(z) = \left.\frac{0.9586\,s+1}{0.9586\,s/\rho+1}\right|_{s=(2/T_S)((z-1)/(z+1))}. \tag{3.7}$$

Figure 11 shows time response of the controlled system, which gives reference input $R(n)$ (dash line), output Y (solid line), time series $G(n)$ (dotted line), and ratios $F(n)$ (dash-dotted line) of $G(n)$. It gives good performance and zero steady-state errors. Figure 11 shows the considered plant is a large time-lag system. The high order system model is usually used to describe the industry process for replacing pure time delay (e.g., $e^{-T_d s}$) such that conventional analysis and design techniques can be applied [7, 8]. Figure 11 shows the proposed method can be applied to a large time-delayed system.

Final results and four other methods are presented for comparison and show the merit of the proposed method. They are Ziegler-Nichols method [9–12] for finding PI and PID compensators, Zhuang and Atherton [23] for finding PI compensator, and Majhi [7, 8] for finding PI compensator. Parameters of four found compensators are given below:

(1) ZN(PI): $K_p = 0.585$ and $K_i = 0.0305$;

(2) ZN(PID): $K_p = 0.77256$,$K_i = 0.05088$, and $K_d = 4.9135$;

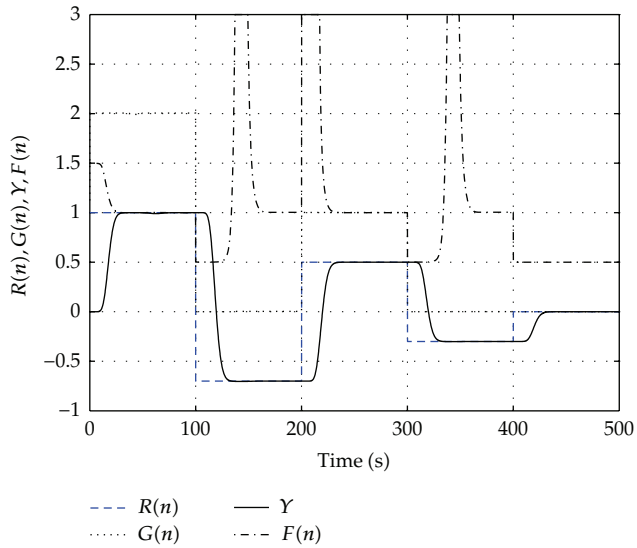

Figure 11: Time responses of Example 3.3 with $C(z)$ for $\beta = 0.5$; $T_S = 25$ ms.

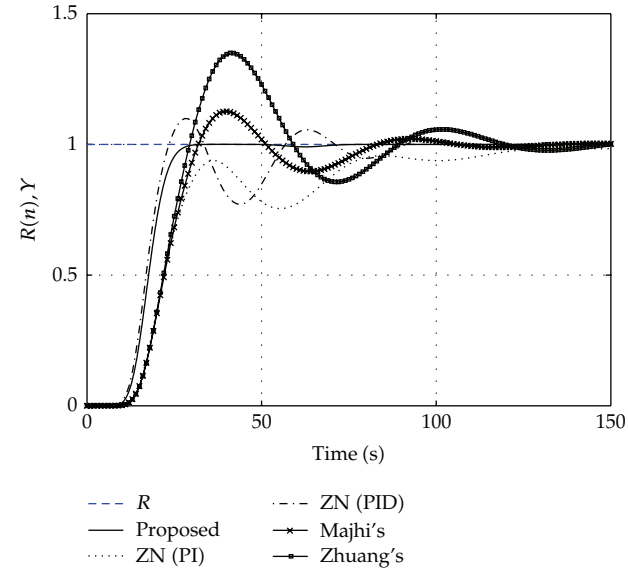

Figure 12: Time responses of Example 3.3 using different control methods.

(3) Majhi's(PI): $K_p = 0.5097$ and $K_i = 0.0443$;

(4) Zhuang's(PI): $K_p = 0.473$ and $K_i = 0.058$.

Time responses are shown in Figure 12. Table 3 gives integration of absolute error (IAE) and integration of square error (ISE) of them. From Table 3 and Figure 12, one can see that the proposed method gives better performance than those of other methods.

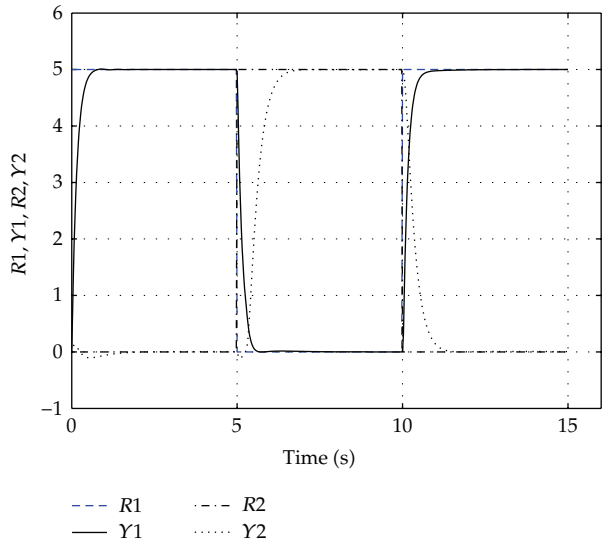

Figure 13: Time responses of Example 3.4 for $\beta = 0.5$ and $T_S = 25$ ms.

Table 3: IAE and ISE errors of Example 3.3 using different control methods.

Methods	Proposed	ZN(PI)	ZN(PID)	Majji's	Zhuang's
ISE	15.7313	21.2271	16.2160	20.1908	21.8142
IAE	18.0892	32.7084	22.9707	26.8295	32.9125

Example 3.4. Consider a gas turbine engine with plant transfer function matrix [24–26]:

$$P_4(s) = \frac{1}{\Delta(s)} \begin{bmatrix} 2533 + 1515.33s + 14.9s^2 & 1805947 + 1132094.7s + 95150s^2 \\ 12268.8 + 8642.68s + 85.2s^2 & 2525880 + 1492588s + 124000s^2 \end{bmatrix}, \tag{3.8}$$

where $\Delta(s) = 2525 + 3502.7s + 1357.3s^2 + 113.22s^3 + s^4$. It is a 2×2 multivariable plant. The steady-state gain of open loop $P_4(s)$ is in the form of

$$P_4(0) = \begin{bmatrix} 1.00316 & 715.2265 \\ 4.85893 & 1000.3485 \end{bmatrix}. \tag{3.9}$$

A pre-compensating matrix $P_4^{-1}(0)$ is first applied to decouple the plant in low-frequency band. Then, two digital filters are used in the diagonal to filter outputs of two time series for speeding up transient responses. They are in the form of

$$\begin{aligned} C_1(z) &= \left.\frac{0.75s + 1}{0.15s + 1}\right|_{s=(2/T_S)((z-1)/(z+1))}, \\ C_2(z) &= \left.\frac{0.60s + 1}{0.25s + 1}\right|_{s=(2/T_S)((z-1)/(z+1))}, \end{aligned} \tag{3.10}$$

where $T_S = 25\,\text{ms}$ is the sampling period. Figure 13 shows time responses of this controlled system for $\beta = 0.5$. It shows that the proposed control scheme can be applied to the multivariable feedback control system also.

4. Conclusions

In this literature, a new nonlinear digital controller has been proposed for analyses and designs of industry processes. They are sampled-data feedback control systems. It was applied to four simple and complicated numerical examples to get good performance and zero steady-state errors. No integrations of tracking errors are needed to get zero steady-state errors. Lead compensations are also found by another numerical time series to speed up the system responses on the on-line adjusting manner. From simulation and comparison results with other famous control methods, it can be seen that the proposed method provides another possible control scheme for sampled-data feedback control systems, and it is worthwhile to find other regulation $F(n)$ to get better performance.

References

[1] K. Ogata, *Discrete-Time Control System*, Prentice-Hall, Englewood Cliffs, NJ, USA, 1994.

[2] B. C. Kuo, *Digital Control Systems*, 1995.

[3] C. L. Phillips and H. T. Nagle, *Digital Control System Analyses and Designs*, Prentice-Hall, Englewood Cliffs, NJ, USA, 1994.

[4] G. F. Franklin and J. D Powelll, *Feedback Control Dynamics*, Addison-Wesley Publishing Company, 1986.

[5] G. F. Franklin, J. D. Powell, and M. L. Workman, *Digital Control of Dynamics*, Ellis-Kagle Press, Half Moon Bay, Calif, USa, 2006.

[6] G. S. Buja and A. Souliaev, "A variable structure controller," *IEEE Transactions on Automatic Control*, vol. 33, no. 2, pp. 206–209, 1988.

[7] S. Majhi and D. P. Atherton, "Autotuning and controller design for processes with small time delays," *IEE Proceedings D*, vol. 146, no. 5, pp. 415–425, 1999.

[8] S. Majhi, "On-line PI control of stable processes," *Journal of Process Control*, vol. 15, no. 8, pp. 859–867, 2005.

[9] J. G. Ziegler and N. B. Nichols, "Optimum settings for automatic controllers," *Transactions of ASME*, vol. 65, pp. 759–768, 1942.

[10] K. J. Åström and T. Hägglund, "Revisiting the Ziegler-Nichols step response method for PID control," *Journal of Process Control*, vol. 14, no. 6, pp. 635–650, 2004.

[11] K. J. Åström and C. C. Hang, "Towards intelligent PID control," *Automatica*, vol. 28, pp. 1–9, 1991.

[12] K. J. Åström and T. Hägglund, "Automatic tuning of simple regulators with specifications on phase and amplitude margins," *Automatica*, vol. 20, no. 5, pp. 645–651, 1984.

[13] K. K. Tan, T. H. Lee, and X. Jiang, "Robust on-line relay automatic tuning of PID control systems," *ISA Transactions*, vol. 39, no. 2, pp. 219–232, 2000.

[14] K. K. Tan, T. H. Lee, and X. Jiang, "On-line relay identification, assessment and tuning of PID controller," *Journal of Process Control*, vol. 11, no. 5, pp. 483–496, 2001.

[15] W. K. Ho, C. C. Hang, and L. S. Cao, "Tuning of PID controllers based on gain and phase margin specifications," *Automatica*, vol. 31, no. 3, pp. 497–502, 1995.

[16] C. A. Monje, Y. Q. Chen, B. M. Vinagre, D. Xue, and V. Feliu, *Fractional Order Systems and Controls—Fundamentals and Applications*, Springer, 2010.

[17] M. Li, "Fractal time series—a tutorial review," *Mathematical Problems in Engineering*, Article ID 157264, 26 pages, 2010.

[18] H. Sheng, Y. Q. Chen, and T. S. Qiu, *Fractional Processes and Fractional Order Signal Processing*, Springer, 2012.

[19] C. Tricaud and Y. Q. Chen, *Optimal Mobile Sensing and Actuation Policies in Cyber-Physical Systems*, Springer, 2012.

[20] M. Li and W. Zhao, "Visiting power laws in cyber-physical networking system," *Mathematical Problems in Engineering*, vol. 2012, Article ID 302786, 13 pages, 2012.

[21] Y. Luo, Y. Chen, H. S. Ahn, and Y. Pi, "Fractional order robust control for cogging effect compensation in PMSM position servo systems: stability analysis and experiments," *Control Engineering Practice*, vol. 18, no. 9, pp. 1022–1036, 2010.

[22] C. Tricaud and Y. Chen, "An approximate method for numerically solving fractional order optimal control problems of general form," *Computers & Mathematics with Applications*, vol. 59, no. 5, pp. 1644–1655, 2010.

[23] M. Zhuang and D. P. Atherton, "Automatic tuning of optimum PID controllers," *IEE Proceedings D*, vol. 140, no. 3, pp. 216–224, 1993.

[24] D. Q. Mayne, "The design of linear multi-variable systems," *Automatics*, vol. 9, pp. 201–207, 1973.

[25] D. Q. Mayne, "Sequential design of linear multivariable systems," *Proceedings of the Institution of Electrical Engineers*, vol. 126, no. 6, pp. 568–572, 1979.

[26] T. S. Tsay, "A sequential design method for multivariable feedback control systems," *WSEAS Transactions on Systems*, vol. 8, no. 12, pp. 1294–1304, 2009.